The use of Preston equation to determine material removal during lap-grinding with electroplated CBN tools

Mariusz Deja

Gdańsk University of Technology, Faculty of Mechanical Engineering and Ship Technology, Department of Manufacturing and Production Engineering, 11/12 G. Narutowicza Str., Gdańsk, PL 80-233, Poland

ARTICLE INFO

ABSTRACT

Grinding executed in a lapping configuration is an alternative finishing process benefiting from both grinding and free-abrasive machining, while minimizing the heat effect impact. Electroplated tools can be effectively used in different abrasive processes, including high-speed grinding, however, the assessment of machining performance over time is a key factor in their correct use to achieve satisfactory technological results. In conventional grinding, bigger grain-coverage provides better results due to the higher bonding strength of grains. In lap-grinding, fracturing and crushing of the abrasive particles initially covered by the plating result in a suspension which is typically dosed continuously in free-abrasive machining. Due to this, the process transforms from two-body (grinding) to three-body abrasion (free abrasive machining) which may result in reduced grinding performance approaching asymptotically a specific value while improving surface finish. The main aim of the presented study is the evaluation of electroplated CBN tools used in lap-grinding of 40H alloy steel workpieces whose hardness was 54 HRC. The obtained results and observations of the working surface of CBN wheels and workpieces allowed for the identification of the wear characteristics for three nickel plating thicknesses corresponding to 35%, 50% and 65% of the nominal CBN crystal size and for specific process parameters. The surface roughness Ra parameter decreased gradually from the initial value 1.9 μm to the values below 0.7 μm for bigger B107 grains and for all plating thicknesses. For smaller B64 grains, the surface roughness and waviness parameters reached similar values to those obtained for the larger B107 grains at corresponding processing times. The lowest value of Ra parameter below 0.4 μm was obtained for B64 grains and for the thinnest plating but with a 50% reduction in material removal comparing to B107 grains. The Preston equation was employed to calculate the material removal as a function of time under variable process conditions in the machining zone due to the tool wear. This attempt extended the range of the material removal modeling, despite the fact that the electroplated wheels were subject to wearing down resulting in the gradual reduction in the efficiency, as well as in the change of the working conditions in the workpiece-tool contact zone.

1. Introduction

Abrasive processes are typically used to reduce surface roughness and achieve close tolerances. Lapping is a basic flattening process carried out on a workpiece surface using a single tool - single-sided lapping [1,2], or simultaneously on two plane-planar surfaces using two tools - double-sided lapping [3]. It is realized using loose abrasive micrograins mixed with a carrier in the form of a suspension or paste delivered to the processing area [4]. Low cutting speeds, typically below 5 m/s, in combination with small height reduction obtained at the time, minimize the thermal effects and the risk of grinding burns or subsurface damage. Moreover, lapping can minimize or eliminate surface defects, shape

errors and subsurface damage resulting from previous operations [5].

In grinding, more heat is generated, which results in surface defects, such as burns, and near-surface microstructural changes [6]. Grinding may also cause work-hardening without phase transformation at low depths of cut and cutting speeds [7]. This alternative method of grinding eliminates the disadvantages associated with grinding hardening caused by the temperature, but requires the accurate selection of process parameters to ensure that a large fraction of the grinding energy falls on the material's plastic deformation. Other processes, such as fine grinding [8] or chemical mechanical polishing (CMP) [9] can also be applied to obtain a fine surface finish. Different microgroove structures can be developed on the surface of difficult-to-cut materials using ultrafast laser
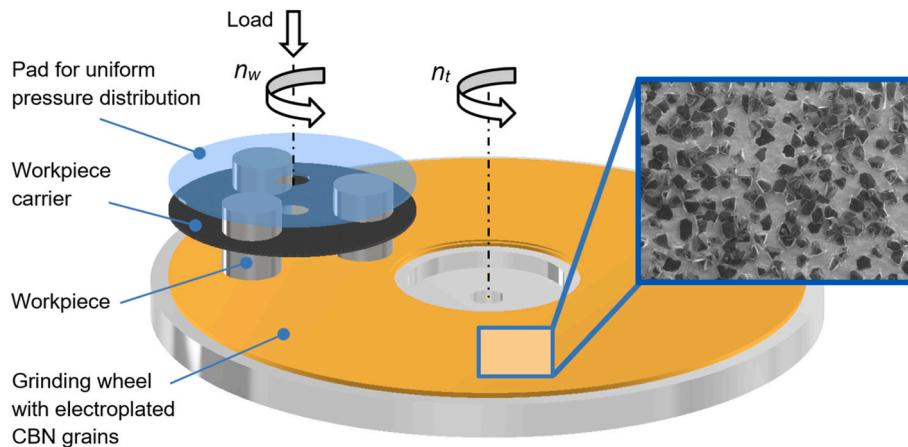
Fig. 1. Schematic drawing of the implemented process with the kinematics of single-disc lapping with the main elements of the executive system and kinematic parameters.

microprocessing, e.g. to fabricate super hydrophilic surface on alumina ceramic [10].

Lap-grinding [11], i.e. grinding with lapping kinematics, is another alternative finishing process that possesses the advantages of grinding (high efficiency) and lapping (good flatness) with minimal heat effect [12–14]. This keeps the thermal energy transferred to the samples and tool at a low level, minimizing residual stresses. Other advantages of lap-grinding with regard to the residual stresses and surface integrity are the tension-free workpiece holding in the separators as well as uniform load distribution during processing [15]. This is due to the lapping configuration when the machined surface is also the machining base without the sample being rigidly fixed. In lap-grinding, lapping discs are replaced by grinding wheels [16], making it a cleaner and more efficient technology, as presented in [15,17] for sapphire and oxide ceramics. It is usually performed at higher cutting speeds compared to lapping, especially in double-sided kinematical configuration [18]. A single-sided kinematical configuration is more suitable for electroplated tools mainly due to the lower values of process parameters, such as speeds and loads [19,20]. The electroplated tools are characterized by almost no restrictions in shape but they have a limited tool life due to a single layer of diamond [21,22] or cubic boron nitride (CBN) grains [23,24] held in the nickel alloy or Fe–Zn matrix [25]. The assessment of grinding performance over time is a key factor in the correct use of electroplated tools to achieve a satisfactory technological effect [26]. The influence of electroplated tool wear on acoustic emission signal and workpiece surface quality during mill-grinding was analyzed in [27]. The data presented in [28] confirmed that the analysis of audible signals can be used as a quick indicator of technological effects in processes which use electroplated tools. The wear of single-layer electroplated CBN grinding wheels was investigated in [29,30]. The experiments conducted with wheels containing different abrasive grain sizes and the height of the nickel plating using three nickel plating thicknesses corresponding to 35%, 50% and 65% of the nominal CBN crystal size showed the influence of the wear process on the wheel topography and grinding behavior. Surprisingly and despite the increased loss of crystals, low tool wear and a high G-ratio were obtained for grinding wheels with a thinner bond [30]. Due to these results, it was decided to use in the previous work on diamond grains and ceramic samples [14] and also in the presented study on CBN grains and steel samples the same three thicknesses of nickel plating as in [30].

The use of electroplated CBN and diamond tools in lapping configuration was shown in [31,32]. Obtained results confirmed that the plating thickness exerted a significant effect on the tool wear influencing the removal rate and surface finish, as the abrasive protrusion height is a core parameter of abrasive tools, and it is also a principal parameter for modeling and simulation of the surface topography of abrasive tools

[33]. The influence of the grains' dimension and the height of their coverage by the nickel plating on the wear of electroplated diamond tools was studied in [34]. In conventional grinding, bigger grain-coverage provided better grinding effects due to the higher bonding strength of grains [35,36]. In lap-grinding, fracturing and crushing of crystal particles covered by the thinnest plating formed a suspension which is typically dosed continuously in free-abrasive machining [34]. Due to this, the process transforms from two-body (grinding) to three-body abrasion (free abrasive machining), which may result in reduced grinding performance while improving surface finish [37].

The main aim of the presented study is the evaluation of electroplated CBN tools used for machining 40H alloy steel workpieces whose hardness was 54 HRC. Conducted experiments and obtained technological effects identified the wear of wheels with a galvanic coating of different heights containing bigger and smaller CBN grains, B107 and B64 respectively. The formula derived from Preston's equation was developed to calculate the material removal as a function of time, taking into account the change in the nominal pressure and variable conditions caused by the wear of applied tools. Observations of the working surface of CBN wheels and workpieces identified the wear characteristics for specific plating thicknesses.

The obtained results fill the research gap related to the use of electroplated CBN tools especially in flat grinding with lapping kinematics. They indicate the influence of grain size and binder thickness on machining efficiency and surface finish, enabling wider production of such tools. A decreasing machining efficiency over time, typical for machining with the use of electroplated tools due to the tool wear, makes modeling the height reduction difficult. The adopted modeling methodology using an exponential function allows to determine the maximum theoretical height reduction as the sample height tended asymptotically to a specific value, corresponding to the nature of machining with this type of tools. The Preston equation allowed to extend the range of the material removal modeling. The novel use of the Preston equation consists in the employment of the coefficient related to the wear resistance of the tool. It increases with the growing plating thickness corresponding to the stronger fixing of the grains in the binder. The novel attempt to the wear characteristics and systematization of the course of machining with electroplated CBN wheels related the process transformation from two-body (grinding) to three-body abrasion (free abrasive machining) for specific plating heights is also presented in this article.

2. Materials and methods

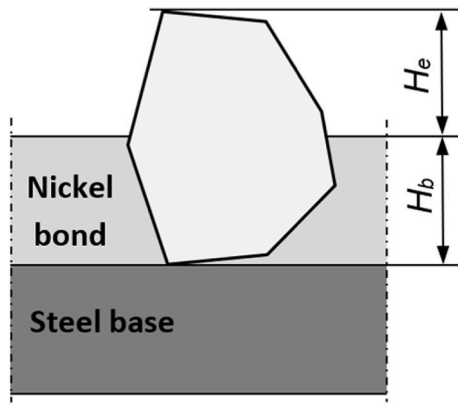The process was conducted in a kinematical configuration presented

Fig. 2. The grain exposure H_e above the nickel bond of H_b thickness.

Table 1
Parameters for machining steel samples with electroplated CBN tools.

Process entity	Parameter	Symbol	Value/name	Parameter type: X – independent G – constant
Tool	External radius	r_e	180 mm	g_1
	Internal radius	r_i	45 mm	g_2
	Abrasive	B	Cubic boron nitride (CBN)	g_3
	Abrasive dimension	d_g	64 μm; 107 μm	x_1
	Number of particles per unit area	C_{B64}; C_{B107}	130 mm^{-2}; 70 mm^{-2}	g_4
	Bonding	Ni	Nickel	g_5
	Relative height of the plating	T_b	35%; 50%; 65%	x_2
Parameters	Wheel velocity	n_t	60 min^{-1}	g_6
	Workpiece carrier velocity	n_w	121 min^{-1}	g_7
	Load	p	9 kPa; 14 kPa	x_3
	Duration of a single test (continuous processing)	Δt_{B64}; Δt_{B107}	270 s; 90 s	g_8
	Maximum number of tests	i_{B64}; i_{B107}	3; 9	g_9
	Processing time	t_p	$t_p = i\Delta t$	x_4
Lubrication	Grain carrier	VECO Megol WR 10	Cutting fluid	g_{10}
	Kinematic viscosity at 40 °C	ν	10.5 mm^2 s^{-1}	g_{11}
	pH	pH	5.60	g_{12}
	Dosage	$\dot{Q}_{lub}$	3 ml/min	g_{13}
Samples	Material	40H	alloy steel	g_{14}
	Hardness	HRC	54 HRC	g_{15}
	Cylindrical dimension	d_w	Ø34	g_{16}
	Linear dimension before experiments	h_{w0}	20 mm	g_{17}
	Roughness parameter before experiments	Ra	1.9 μm	g_{18}

schematically in Fig. 1. A workpiece carrier and a tool had independent drives allowing accurate setting of the required rotational velocities n_t and n_w, respectively. Steel surfaces were machined while being in contact with the working surface of tools with CBN particles of two sizes:

B107 and B64 covered by plating of different heights. According to ISO designation (ISO 6106–2005), the grain dimensions d_g were 107 μm and 64 μm for B107 and B64 particles, correspondingly. The absolute height of the plating H_b influences directly the grain exposure H_e above the bond, which is schematically shown in Fig. 2. The relative height of the plating in relation to the grain dimension can be formulated as:

$$T_b = \left(\frac{H_b}{d_g}\right)100\% \tag{1}$$

where: T_b – the relative height of the plating in %, H_b - the absolute height of the plating in μm, d_g –grain dimension in μm.

All the process conditions related to the wheel, parameters, lubricant and samples are given in Table 1. The cutting fluid was used as a lubricant and a carrier of fractured grains and chips removed from the steel samples. For both grain dimensions $d_g = 107$ μm and 64 μm, three relative heights $T_b = 35\%$, 50% and 65% of the grain-coverage were used, which corresponded to the thinnest, medium and thickest plating, respectively. Thus, a total of six types of tools were tested experimentally. A digital micrometer (Mitutoyo, Kawasaki-shi, Japan) with a 1 μm resolution was used for the sample height measurements. A contact profiler Hommel Tester T1000 (HOMMEL ETAMIC, Villingen-Schwenningen, Germany) was used for measuring the surface roughness and waviness parameters. The output data were measured three times at different locations on each sample. For the three samples, the total number of height, roughness and waviness measurements was therefore 9. The state of the working surface of the tools was examined by environmental scanning electron microscope (Philips-FEI XL 30 ESEM) after all experiments were completed, and the tools were cut into smaller pieces to allow microscopic observation. Fragments of tools cut from the middle zone of the working tool surface were subjected to microscopic observations, which is schematically shown in Fig. 1.

The methodology of planning the experiment (Fig. 3), takes into account the independent variables X, constant G and disturbing factors J as well as dependent variables Y, such as.

  y$_1$ – height reduction (linear material removal) ΔH;
  y$_2$ – surface roughness parameter Ra;
  y$_3$ – surface waviness parameter Wa.

Selected independent variables **X** and constant factors **G** are listed in Table 1. The main disturbing factors **J** were assumed as.

  j$_1$ – change in the areal grain concentration and in the number of active grains;
  j$_2$ – variation of the physical-mechanical properties of the tool and the steel samples;
  j$_3$ – uneven dosage and distribution of the slurry on the working surface of the tool.

The tool wear by removing and crushing grains into smaller particles increases their areal concentration and the number of active grains changing the properties of a tool, especially reducing its cutting ability. This was considered in the model of material removal by using an exponential function, as the sample height tended asymptotically to a specific value. After changing the tool properties by increasing the nominal pressure, the employment of the Preston equation allowed to extend the range of the material removal modeling. Developed equations allowed a very good curve fitting before and after the pressure change and despite the fact that the electroplated wheels were subject to wearing down resulting in the gradual reduction in the efficiency as well as in the change of the working conditions in the workpiece-tool contact zone.
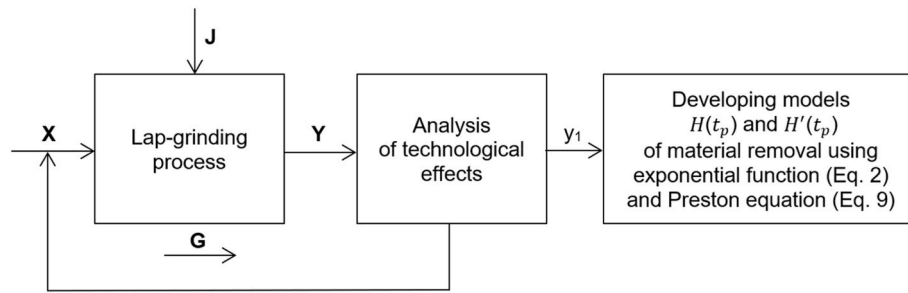
Fig. 3. Scheme of the lap-grinding experiment planning methodology: **X** – independent variables, **Y** – dependent variables, **G** – constant factors, **J** – disturbing factors.

3. Outcomes from experimental tests

In the experimental tests, the influence of the height of the grain-coverage H_b, the machining time t_p, and the unit pressure p on the achieved technological effects, i.e. material removal rate, surface roughness and waviness, was analyzed using the machining parameters presented in Table 1 and the kinematics of single-disc lapping shown in Fig. 1.

3.1. Reduction of the sample height

Tests with the use of wheels with B107 grains were carried out with constant kinematic parameters and for two values of the unit pressure: $p_1 = 9$ kPa for $t_p \leq 270$ s, and $p_2 = 14$ kPa for $t_p > 270$ s for three relative plating heights, i.e. $T_b = 65\%$, 50%, and 35%. After the first series, the load was increased (for $t_p > 270$ s) as the effectiveness of machining clearly tended to decrease over time in the first series (for $t_p \leq 270$). The load increase after 270 s of processing significantly increased the height reduction (Fig. 4), similar to Al_2O_3 ceramics and D107 diamond grains [34]. The increasing tendency was observed for each plating thickness, but the biggest relative plating height ($T_b = 65\%$) resulted in the lowest height reduction of the steel samples - Fig. 4 a. The thickest nickel coating caused the grains to be more deeply immersed in the binder, but also less exposed, protecting grain pullouts. Thus, the progressive decrease in the effectiveness of material removal rate indicates dulling of abrasive particles as the dominant type of wear reducing the process efficiency, and that two-body abrasion characteristic for grinding dominated during processing with the thickest bond ($T_b = 65\%$) with B107 grains.

Higher exposure of abrasive grains in a thinner bond for $T_b = 50\%$ resulted in the highest material removal for both series conducted under $p_1 = 9$ kPa and $p_2 = 14$ kPa unit pressures – Fig. 4 b. Better abrasive properties made it possible to extend the effective tool usage to 810 s, compared to 630 s for the tool with the thickest plating, despite the naturally weaker grains embedment in a nickel bond of an intermediate height. The greater exposure allowed the grits to be removed more easily from the bond, helping them to break. Fracturing and crushing of bigger grains helped to cut the material by an increased number of smaller particles in a suspension (more loose grains), activating three-body abrasion typical for free-abrasive machining.

After 270 s of processing in the first series, the material removals were at similar levels for tools with the thickest (Fig. 4 a) and thinnest bond (Fig. 4 c), but they were lower than for the intermediate one (Fig. 4 b). The load increase after 270 s of processing increased the height reduction for all tools, but it was most noticeable for the wheel with the thinnest bond. The effective tool usage of this tool was 810 s with the final material removal higher than for the thickest bond, and slightly lower than for the intermediate one, which was likewise used effectively for 810 s. Obtained results indicate that two-body abrasion dominated for the thickest bond ($T_b = 65\%$), lap-grinding for the intermediate bond ($T_b = 50\%$), and free abrasive machining for the thinnest bond ($T_b = 35\%$).

Tests using the wheels with B64 grains were also carried out with constant kinematic parameters but only for one value of the unit pressure $p_1 = 9$ kPa, with the total processing time $t_p = 810$ s. Three subsequent tests lasting 270 s were performed also for three relative plating heights, i.e. $T_b = 65\%$, 50%, and 35% but the applied load was not increased during experiments. Surprisingly, the effectiveness of wheels with smaller B64 grains (Fig. 5) was better than that for bigger B107 grains (Fig. 4), with the highest material removal obtained also for the intermediate bond height ($T_b = 50\%$). B64 grains with the thickest bond ($T_b = 65\%$) allowed obtaining similar material removal as for the intermediate one (Fig. 5), and almost two times higher than for B107 grains (Fig. 4a). This was due to the fact that lower adhesion forces between the smaller B64 grains and nickel bond along with higher areal concentration allowed their easier removal even from the thickest bond and, as a result, a greater share of loose grains in processing and higher material removal were observed. However, the thinnest bond $T_b = 35\%$ caused the B64 grains to be removed too easily from the binder and the machining zone alike, and consequently, the smallest material removal was obtained – Fig. 5. Larger B107 grains, due to higher adhesion forces, were more firmly fixed even in the thinnest binder (bigger contact area between the grain and bond), which did not allow their easy removal from the machining zone but it did allow the formation of an abrasive suspension. Consequently, a material removal twice as high (Fig. 4 a) as for the smaller B64 grains (Fig. 5) was achieved. Results showed that machining with B64 grains was conducted under the three-body typical abrasion regime, mainly due to the weaker grains embedding in the binder which led to their easier removal and formation of an abrasive suspension.

The achieved values of material removal rates (MRR) for all tools and machining conditions are summarized in Fig. 6. It is clearly visible that the intermediate bond height ($T_b = 50\%$) allowed to achieve the highest efficiency for both grain sizes. The thinnest plating ($T_b = 35\%$) was more effective than the thickest plating ($T_b = 65\%$) for larger B107 grains with the opposite situation for smaller B64 grains.

3.2. Surface roughness and waviness

Reduction in the surface roughness is clearly visible for all sizes of grains and bond thickness – Fig. 7, Fig. 8. For bigger B107 grains, the first three tests T1 ÷ T3 were conducted under the pressure $p = 9$ kPa ($t_p \leq 270$ s), and subsequent tests T4 ÷ T9 under the pressure $p_2 = 14$ kPa ($t_p > 270$ s). Each test lasted 90 s. After the initial T1 test, the values of surface roughness and waviness parameters strictly depended on the grain exposure. In line with the expectations, higher surface roughness was obtained for a bigger exposure, i.e. for $T_b = 35\%$. After 270 s of machining, i.e. after the third test T3, this tendency reversed as the best surface finish was achieved also for the thinnest plating, and the worst surface finish for the thickest one ($T_b = 65\%$). It confirms the observations from the measurements of the material removal, that thinner plating helps the removal and fracture of grains into smaller particles,
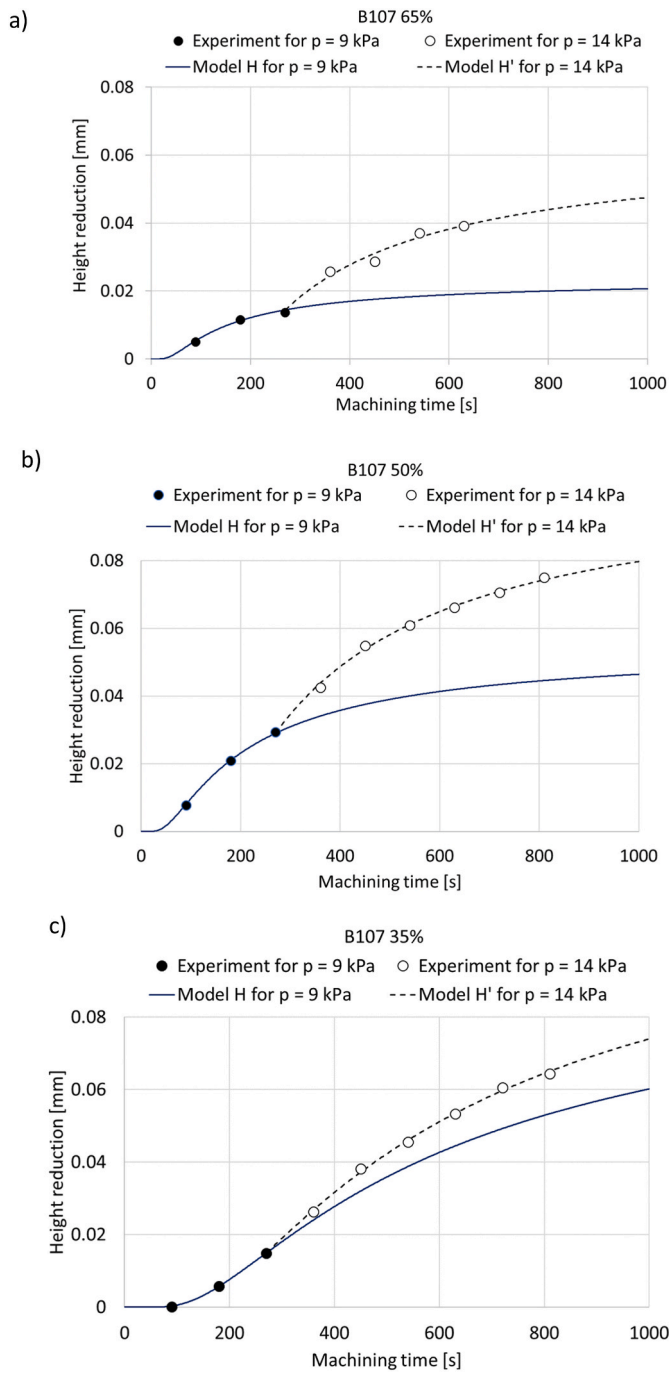
a)

b)

c)

Fig. 4. Calculated and experiment-derived material removal of 40H steel samples using electroplated tools with B107 grains and different relative plating heights: a) $T_b = 65\%$, b) $T_b = 50\%$, c) $T_b = 35\%$; H – an exponential function (Equation (2)), H' – an exponential function with coefficients related to tool wear and pressure increase (Equation (9)), details of the process parameters are presented in Table 1.

increasing their areal concentration and the number of active grains. Due to this, smaller individual forces acted on the abrasive particles as their sum had to be equal to the applied total force. This resulted in a smaller depth of penetration of the abrasive particles into the workpiece surface and, in turn, in lower surface roughness. The reverse is the case with the thickest plating when the grains were more firmly held in the bond with the least exposure above it, so the reduction in surface roughness was mainly due to the attrition wear of the grains. As a result, the surface roughness parameters decreased from the initial values but
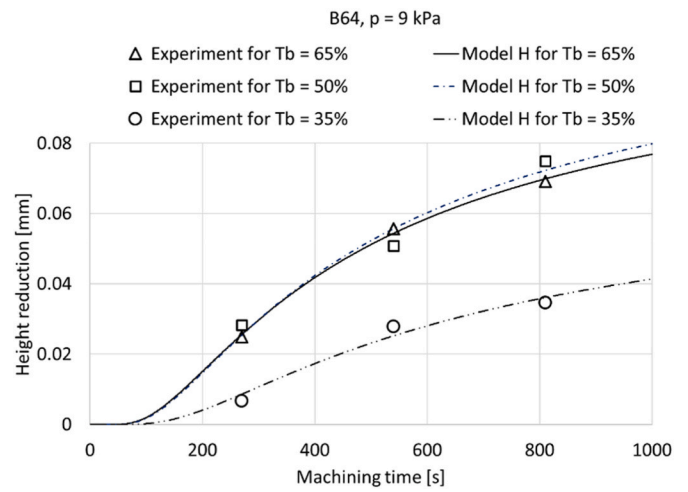

Fig. 5. Calculated and experiment-derived material removal of 40H steel using electroplated tools with B64 grains and different relative plating heights; H – an exponential function (Equation (2)), details of the process parameters are presented in Table 1.
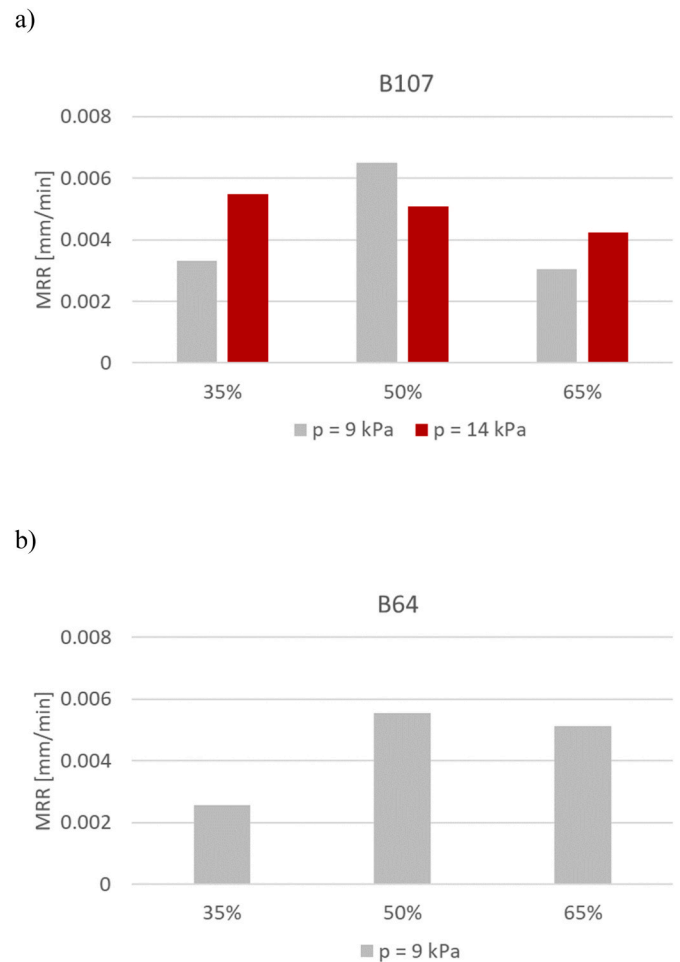
a)

b)

Fig. 6. The average material removal rate (MRR) for B107 (a) and B64 (b) grains.

did not increase even with an increase in the unit pressure after 270 s of machining (after T3 test), which was the case for all bindings – Fig. 7 a. The surface waviness parameters also decreased but with relatively high
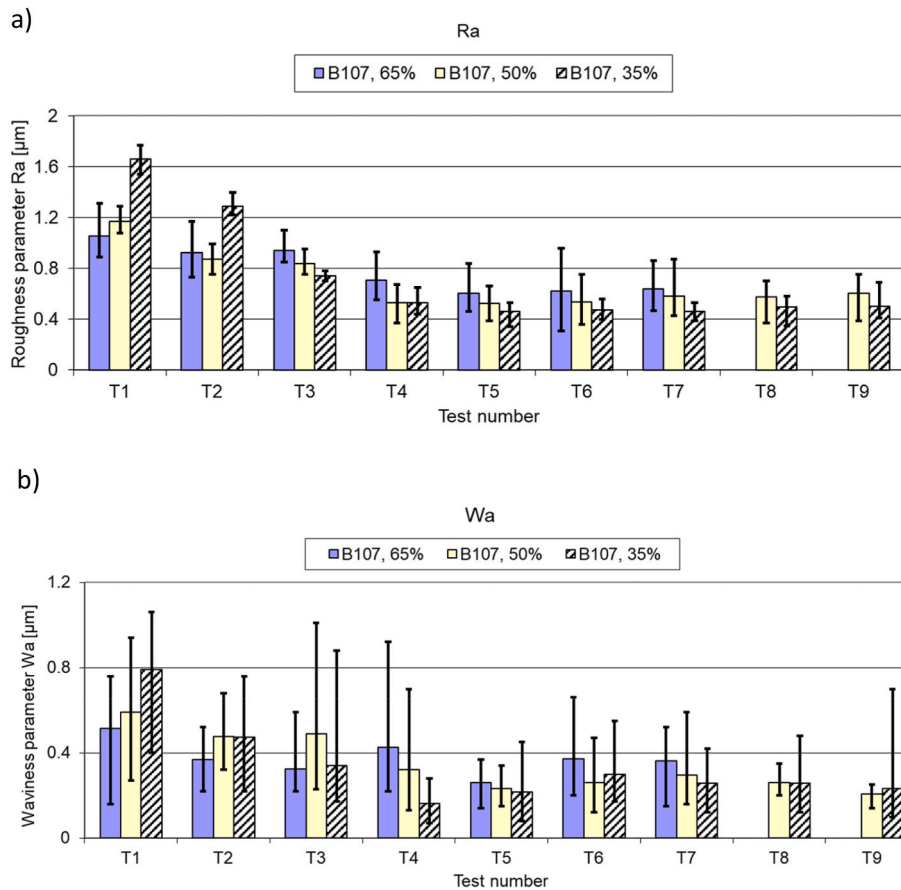
a)

Ra

b)

Wa

Fig. 7. Roughness parameters Ra (a) and waviness parameters Wa (b) after lap-grinding of 40H steel using electroplated tools with B107 grains and different relative plating heights; details of the process parameters are presented in Table 1.

variability and spread in most cases – Fig. 7 b. This may be due to the tension-free workpiece holding, which minimizes the thermal effect and residual stresses but allows the samples to move in the separator hole without being rigidly fixed.

For smaller B64 grains, the surface roughness and waviness parameters (Fig. 8) reached similar values to those obtained for the larger B107 grains (Fig. 7), at corresponding processing times of 270, 540 and 810 s. Each of three subsequent T1 ÷ T3 tests lasted 270 s and was conducted only under the pressure $p = 9$ kPa. The smaller grains did not cause much lower roughness even though their areal concentration was bigger and the pressure did not increase after 270 s. The individual forces acting on the larger number of particles were lower and due to this, they did not help to further crack and fracture the abrasive into smaller particles, as was the case with larger grains. The lowest values of the Ra and Wa parameters were achieved also for the thinnest binder after 810 s of machining, i.e. after the third test T3.

Obtained results confirmed that the same surface roughness can be achieved for different grain sizes, depending, however, on the plating thickness, processing time and process parameters. This is relevant with the results presented in [38] showing that apart from the grain size also the sharpness and the cutting-points density (controlled by dressing conditions) has a great effect on the surface roughness parameters to be achieved.

4. Modeling of the height reduction

As shown in the previous Section, the reduction of the steel samples' height showed a downward trend during all conducted experiments. Due to the tool wear, the maximum reduction of the sample height tended to reach a specific value, with a decreasing machining efficiency

over time which is typical for machining with the use of electroplated tools [21]. The results of the experiments tending asymptotically to a specific value corresponding to the nature of machining with this type of tools [34,39], decided on the choice of an exponential function to fit the points from experiments. The following model of the reduction of the sample height H over processing time t_p was used:

$$H(t_p) = b_1 \cdot e^{\left(b_2/t_p\right)}, t_p > 0 \tag{2}$$

where: b_1, b_2 - parameters calculated during curve fitting.

A horizontal asymptote assumed as the maximum theoretical material removal for the specific conditions is:

$$y_h = b_1. \tag{3}$$

The results from the computation performed in the Matlab R2021a, software with the root mean square error (RMSE) used to show the differences between the experimental and predicted values are presented in Table 2, Figs. 4, and Fig. 5.

The further modeling was based on applying the Preston formula which is generally dedicated to the processes characterized by constant machining conditions, like free-abrasive machining or polishing with a continuous abrasive dosage [40,41]. Nevertheless, Deja [32] used it efficiently in lap-grinding characterized by the changing conditions due to the tool wear. The electroplated wheels were subjected to wearing down resulting in the gradual reduction in the lap-grinding efficiency, as well as in the change of the friction conditions in the workpiece-tool contact zone. On this basis, the general equation describing the reduction of the sample height during machining using the tools with the B107 grains after an increase or decrease in the nominal pressure was
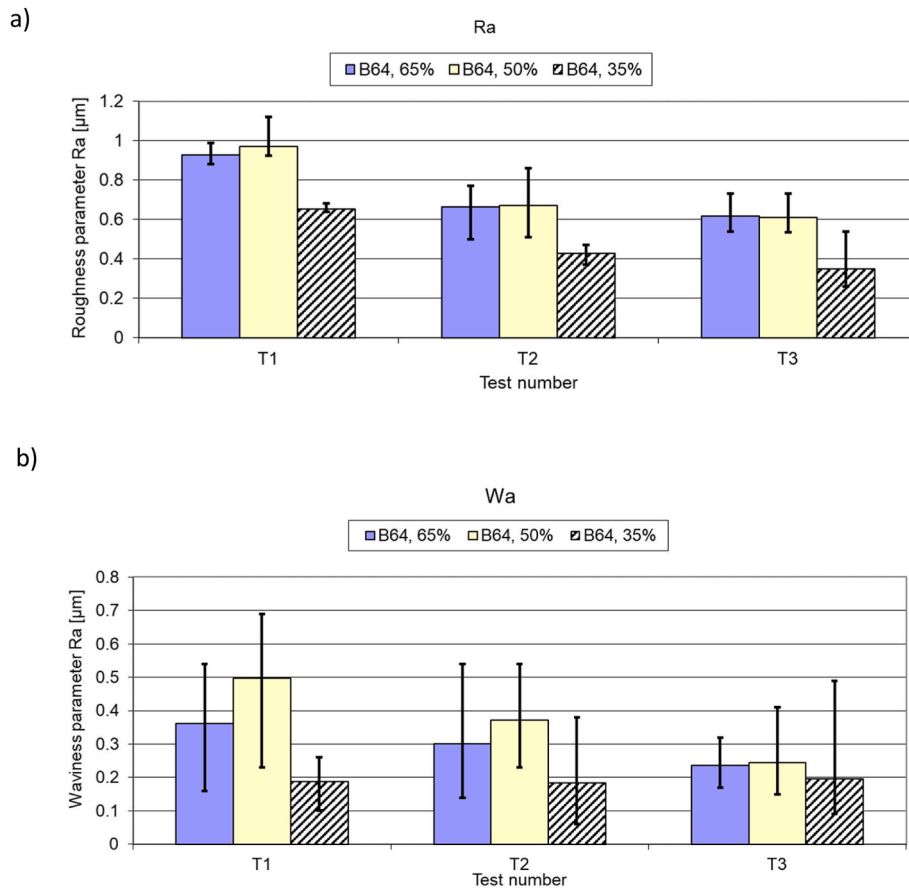
Fig. 8. Roughness parameters Ra (a) and waviness parameters Wa (b) after lap-grinding of 40H steel using electroplated tools with B64 grains and different relative plating heights; details of the process parameters are presented in Table 1.

Table 2
Results from the computation of coefficients of a model H (Equation (2)) for calculating the height reduction of steel samples; details of the process parameters are presented in Table 1.

Abrasive acc. To ISO designation	Relative height of the plating T_b	Processing time t_p, in seconds	Asymptote ($y_h = b_1$) and a maximum theoretical height reduction in millimeters	Model parameter b_2	Root mean square error
B107	65%	270	0.023621	−133.14	0.0005
	50%	270	0.055221	−173.94	7.4745e-06
	35%	270	0.10084	−516.24	0.0001
B64	65%	810	0.11548	−406.91	0.0010
	50%	810	0.12188	−423.03	0.0035
	35%	810	0.073776	−579.68	0.0021

formulated in this research. It was based on the assumption that the continuous wear and an increase in the nominal pressure at the specific processing time t_{p1} resulted in a change of the Preston coefficient k. For a constant relative velocity v (cutting speed), the pressure increase (or decrease) from p_1 to p_2 and the change in the Preston constant from k_1 to k_2 due to the tool wear, the following equations for calculating the reduction of sample height over the time Δt can be used:

$$\frac{\Delta H_1}{\Delta t} = k_1 \cdot p_1 \cdot v, \tag{4}$$

$$\frac{\Delta H_2}{\Delta t} = k_2 \cdot p_2 \cdot v, \tag{5}$$

where: k_1, k_2 - Preston constants for p_1 and p_2 loads, respectively, v – cutting speed.

The resulting material removal ΔH_2 with respect to the initial material removal ΔH_1 can be expressed by the dependency:

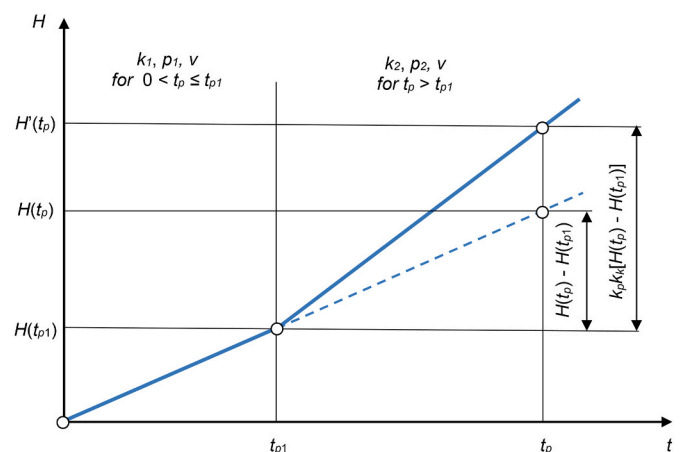$$\frac{\Delta H_2}{\Delta H_1} = k_p \cdot k_k, \tag{6}$$

Fig. 9. The height reduction determined according to the Preston equation during processing before and after changing the load from p_1 to p_2 at t_{p1}.
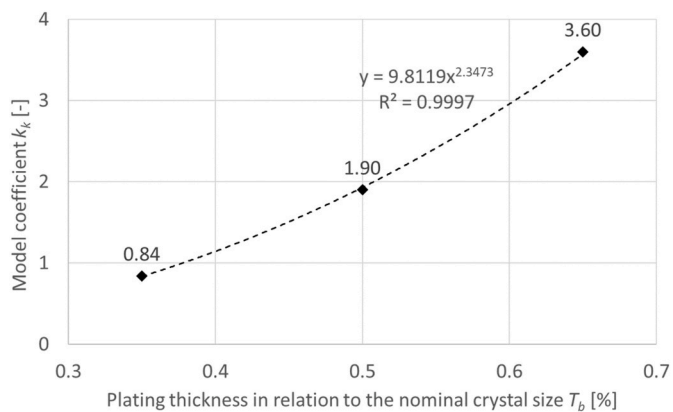
Fig. 10. Coefficient k_k of a model H' (Equation (9)) evaluated for the wheels with B107 grains and different plating thickness.

where:

$$k_p = \frac{p_2}{p_1}, \tag{7}$$

$$k_k = \frac{k_2}{k_1} . \tag{8}$$

The final reduction of the sample height after changing the nominal pressure at the time t_{p1} and due to the variable conditions caused by the wear of applied tools, can be calculated from the equation:

$$H'(t_p) = H(t_{p1}) + k_p \cdot k_k \left[H(t_p) - H(t_{p1}) \right], t_p > t_{p1}, \tag{9}$$

where: H - height reduction calculated using Eq. (2).

Compared to the model derived in [32], Eq. (9) additionally takes into account the change of machining conditions by employing the k_k coefficient related to tool wear. A graphical representation of Equation (9) for the linear relationship, typical for free abrasive machining, is
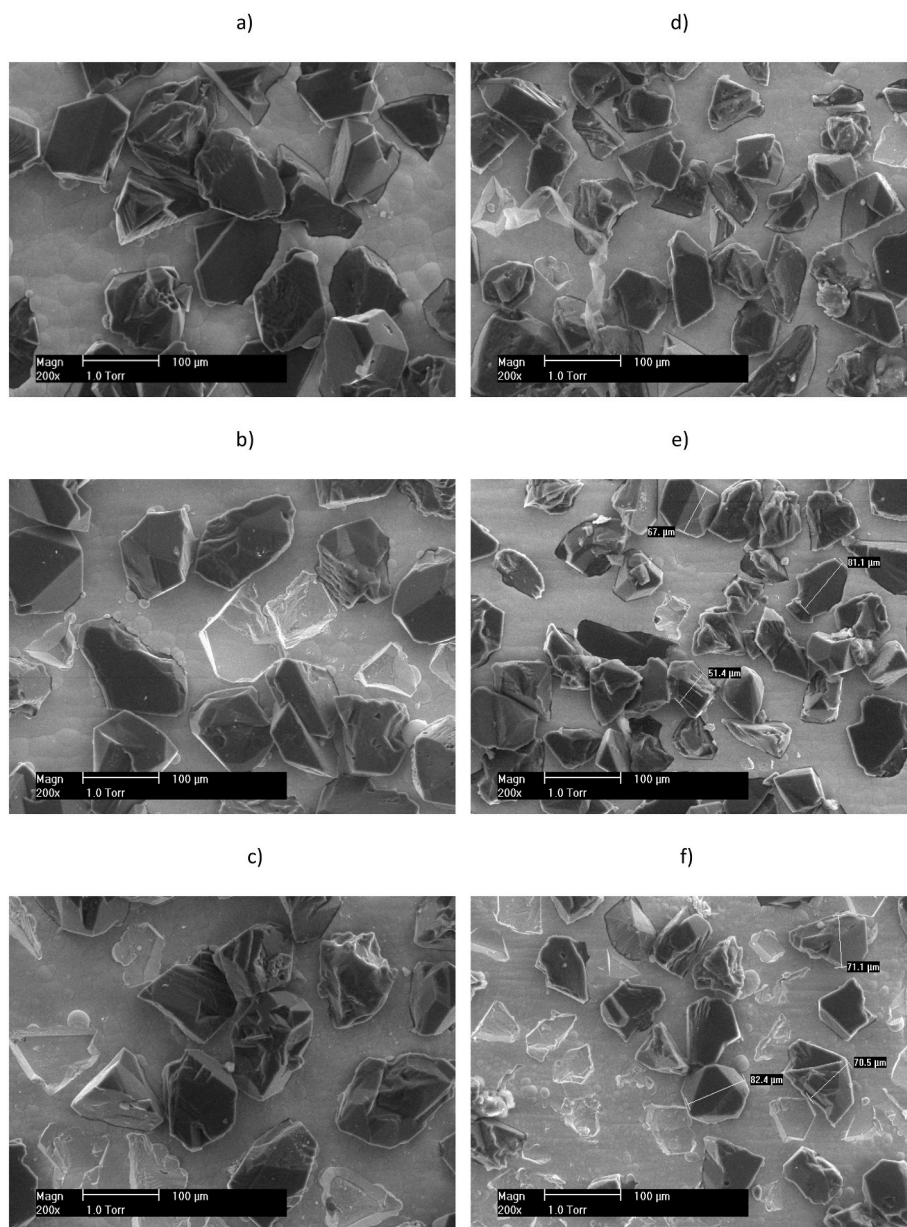

Fig. 11. Fragments of electroplated tools with B107 grits and given plating heights T_b: a) 65%, b) 50%, c) 35%, along with B64 grits and following plating heights T_b: d) 65%, e) 50%, f) 35%.
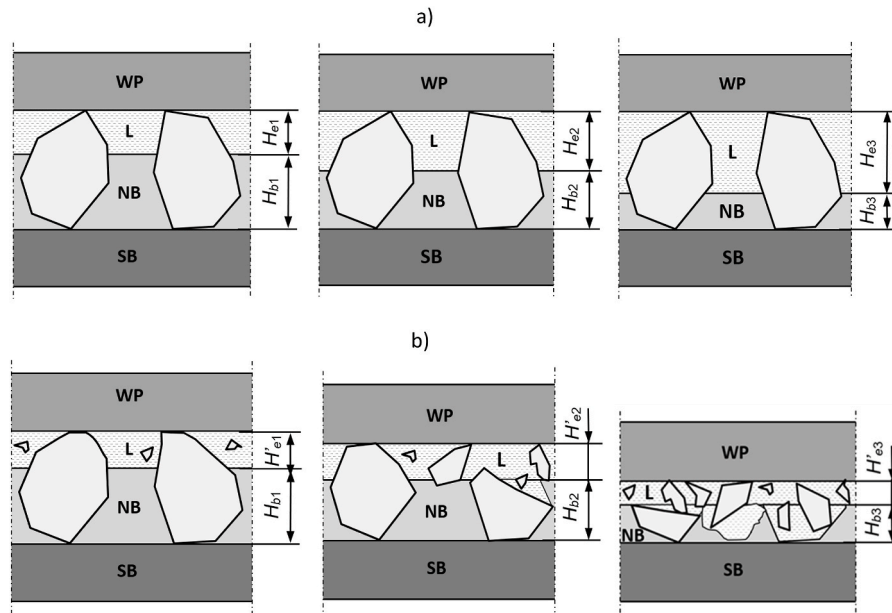
Fig. 12. Influence of the grain plating height ($H_{b1} > H_{b2} > H_{b3}$) on the course of machining and the wear characteristics: a) initial (maximum) and b) reduced grain exposure after machining using electroplated tools
Note: **WP** – workpiece, **L** – lubricant, **NB** – nickel bond, **SB** – steel base.

shown in Fig. 9.

Although in the presented research the height reduction is calculated using the non-linear function (Equation (2)), Eq. (9) allows a very good curve fitting after 270 s of processing ($t_{p1} = 270$ s) and the pressure change from $p_1 = 9$ kPa to $p_2 = 14$ kPa, as seen in Fig. 4. As the value of k_p coefficient is constant ($k_p = 1.56$), the value of k_k coefficient informs about the working conditions in the contact zone between the machined surface and the tool surface. The value of k_k coefficient increases with the increase in the plating thickness corresponding to the stronger fixing of the grains in the binder - Fig. 10. The lowest value of k_k ($k_k = 0.84$) for the thinnest plating and the biggest grains' exposure above the binder, indicates that the pressure change affects the increase in the intensity of the sample height reduction to the lowest extent. This is relevant to the observation from the experiments when the three-body abrasion was activated for the thinner plating before the pressure change, mainly due to the removal of the grains from the working surface of the tool.

5. Discussion

The observations with the SEM microscope showed some wear effects characteristic of applied abrasive particles and grain-coverage - Fig. 11. The analyzed fragments of the working surface of the tools show the cavities in the binder after removing the grits from the nickel plating. It is seen that the number of removed grains (cavities) is the biggest for the thinnest plating and smaller B64 grains - Fig. 11 f. Although the grains were removed, they were still involved in the machining process as loose grains (three-body abrasion) resulting in the effective removal of the steel material. Larger B107 grains were firmly fixed in the thickest bond, which prevented their removal from the working surface of the tool (Fig. 11 a) and, during the machining process, the two-body abrasion dominated. The working conditions changed significantly after the pressure increase, with the late and subsequent initiation of the three-body abrasion. The highest value of the k_k coefficient ($k_k = 3.60$) confirms an increase in the material removal when the pressure is increased (see Fig. 4a).

The process of machining for three different nickel bond heights $H_{b1} > H_{b2} > H_{b3}$ is schematically shown in Fig. 12. A larger initial grain protrusion (Fig. 12 a) promotes their removal with fragmentation, which reduces their exposure H_e and the distance between the tool and

the workpiece (Fig. 12 b). The number of active particles increases with the processing time, but the maximum and average loads per active particle decrease. As a result, the plastic deformation of steel material occurs at smaller depths due to the shallower penetration of abrasive particles into the workpiece. It is expected that for a smaller number of active larger grains of B107 (lower areal concentration), the surface roughness will be higher. The above elucidation was confirmed by experimental results presented in Section 3. The process transformed from grinding treated as two-body abrasion conducted with the thickest bond ($T_b = 65\%$), through lap-grinding for the intermediate bond ($T_b = 50\%$), to conventional lapping treated as three-body abrasion, which was clearly visible for the thinnest bond ($T_b = 35\%$). It is also confirmed by the SEM images of the machined surfaces – Fig. 13. For the thickest bond ($T_b = 65\%$), grinding marks resulting from material removal by grains embedded in the coverage are clearly visible on the steel surface - Fig. 13 a. For the thinnest bond ($T_b = 35\%$), there are cavities in the form of small craters typical for free abrasive machining, with only single grinding marks – Fig. 13 b, c. Moreover, after $t_p = 210$ s (Fig. 13 b) the grinding mark and cavities are bigger than after $t_p = 810$ s (Fig. 13 c). It confirms that the grains are fracturing into smaller pieces with the time of machining, and the dominance of three-body abrasion for the thinnest bond.

The obtained results are limited to grinding with lapping kinematics of steel samples, but the presented methodology can also be applied to other electroplated tools typical of a wide range of shapes but with a limited tool life. However, lap-grinding and electroplated tools were indicated in [42] as the main directions of development of abrasive technologies, especially in relation to the automotive industry sector. In the light of the above, the presented findings along with new tool designs and the developed method of assessment of grinding performance over time may contribute to the further development of abrasive machining. Especially, the employment of the Preston equation may allow to extend the tool life by the possibility of modeling the material removal rate under changeable working conditions. The reported results and wear characteristics can also serve as design guidelines for tool producers and end-users to further extend the limited tool life of electroplated tools.
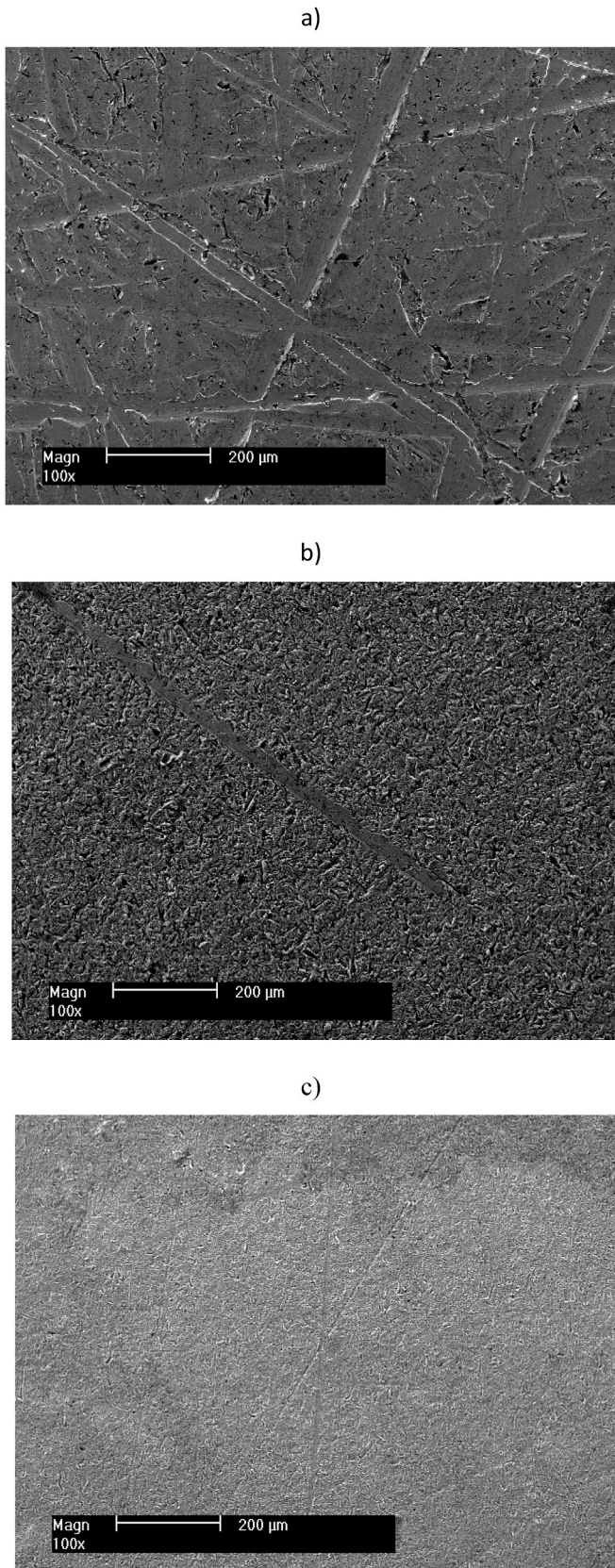
Fig. 13. The SEM images of the steel surfaces after lap-grinding using electroplated tools with B64 grits: a) $T_b = 65\%$, $t_p = 810$, b) $T_b = 35\%$, $t_p = 270$ s, c) $T_b = 35\%$, $t_p = 810$ s.

6. Conclusions

The study on electroplated CBN tools used in this research allowed the following conclusions to be drawn.

- During machining with B107 grains, grinding dominated for the thickest bond ($T_b = 65\%$), lap-grinding for the intermediate bond ($T_b = 50\%$), and free-abrasive machining for the thinnest bond ($T_b = 35\%$);
- Machining with B64 grains was conducted under the three-body abrasion regime typical for lapping (free-abrasive machining) or lap-grinding, mainly due to the weaker grains embedding in the grain-coverage which led to their easier removal;
- Thinner plating helped the grains' removal and fracture into smaller particles, increasing their areal concentration and the number of active grains. This resulted in a smaller depth of penetration of the abrasive particles into the steel workpiece surface and, in turn, in lower surface roughness;
- The maximum reduction of the sample height tended to reach a specific value, with a decreasing machining efficiency over time. Based on this, an exponential function was chosen to fit the points from experiments. A horizontal asymptote of an employed non-linear function can be assumed as the maximum theoretical material removal for the specific working conditions;
- The formula derived from Preston's equation was developed to calculate the material removal as a function of time taking into account the change in the nominal pressure. A novelty in the proposed model, compared to the previous works, consists in considering the change of machining conditions by employing the k_k coefficient related to the tool wear. The value of the k_k model coefficient evaluated for all tools with B107 grains increased with the increase in the plating thickness due to the stronger fixing in the binder.

Author statement

As corresponding author, I <u>Mariusz Deja,</u> hereby confirm that I am the only author who contributed to the paper.

Declaration of competing interest

The authors declare that they have no known competing financial interests or personal relationships that could have appeared to influence the work reported in this paper.

Data availability

Data will be made available on request.

References

[1] L.S. Deshpande, S. Raman, O. Sunanta, C. Agbaraji, Observations in the flat lapping of stainless steel and bronze, Wear 265 (1–2) (2008) 105–116.
[2] M. Deja, Simulation model for the shape error estimation during machining with flat lapping kinematics, in: ASME 2010 International Manufacturing Science and

Engineering Conference, 1, American Society of Mechanical Engineers Digital Collection, 2010, pp. 291–299, https://doi.org/10.1115/MSEC2010-34262.

[3] A. Barylski, M. Deja, Wear of a tool in double-disk lapping of silicon wafers, in: ASME 2010 International Manufacturing Science and Engineering Conference, 1, American Society of Mechanical Engineers Digital Collection, 2010, pp. 301–307, https://doi.org/10.1115/MSEC2010-34323.

[4] X. Zhu, C. Chung, C.S. Korach, I. Kao, Experimental study and modeling of the effect of mixed size abrasive grits on surface topology and removal rate in wafer lapping, Wear 305 (1–2) (2013) 14–22.

[5] T. Shibata, B. Golman, K. Shinohara, M. Otani, T. Uchiyama, Profile analysis of surfaces lapped with diamond particles of several shapes, Wear 254 (7–8) (2003) 742–748.

[6] S. Malkin, C. Guo, Thermal analysis of grinding, CIRP Annals 56 (2) (2007) 760–782.

[7] M. Szkodo, K. Chodnicka-Wszelak, M. Deja, A. Stanisławska, M. Bartmański, The influence of the depth of cut in single-pass grinding on the microstructure and properties of the C45 steel surface layer, Materials 13 (5) (2020) 1040.

[8] Z.J. Pei, A. Strasbaugh, Fine grinding of silicon wafers, Int. J. Mach. Tool Manufact. 41 (5) (2001) 659–672.

[9] C. Park, H. Kim, S. Lee, H. Jeong, The influence of abrasive size on high-pressure chemical mechanical polishing of sapphire wafer, int. J. Precis. Eng. Manuf. Green Technol. 2 (2) (2015) 157–162.

[10] Q. Cao, Z. Wang, W. He, Y. Guan, Fabrication of super hydrophilic surface on alumina ceramic by ultrafast laser microprocessing, Appl. Surf. Sci. 557 (2021), 149842.

[11] J.Y. Shen, X.P. Xu, B. Lin, Y.S. Xu, Lap-grinding of Al_2O_3 ceramics assisted by water-jet dressing metal bond diamond wheel, Key Eng. Mater. 202–203 (2001) 171–176.

[12] V.H. Bulsara, Y. Ahn, S. Chandrasekar, T.N. Farris, Polishing and lapping temperatures, J. Tribol. 119 (1) (1997) 163–170.

[13] J.H. Horng, Y.R. Jeng, C.L. Chen, A model for temperature rise of polishing process considering effects of polishing pad and abrasive, J. Tribol. 126 (3) (2004) 422–429.

[14] A.B. Khoshaim, Z. Xu, I.D. Marinescu, ELID grinding with lapping kinematics, in: Handbook of Ceramics Grinding and Polishing, William Andrew Publishing, 2015, pp. 394–448.

[15] M. Deja, M. List, L. Lichtschlag, E. Uhlmann, Thermal and technological aspects of double face grinding of Al_2O_3 ceramic materials, Ceram. Int. 45 (15) (2019) 19489–19495.

[16] Z. Wang, F. Niu, Y. Zhu, J. Li, J. Wang, Comparison of lapping performance between fixed agglomerated diamond pad and fixed single crystal diamond pad, Wear 432–433 (2019), 202963.

[17] H.M. Kim, R. Manivannan, D.J. Moon, H. Xiong, J.G. Park, Evaluation of double sided lapping using a fixed abrasive pad for sapphire substrates, Wear 302 (1–2) (2013) 1340–1344.

[18] B.J. Cho, H.M. Kim, R. Manivannan, D.J. Moon, J.G. Park, On the mechanism of material removal by fixed abrasive lapping of various glass substrates, Wear 302 (1–2) (2013) 1334–1339.

[19] M. Deja, Correlation between shape errors in flat grinding, J. Vibro Eng. 14 (2) (2012) 520–527.

[20] A. Barylski, M. Deja, Finishing of ceramics in a single-disk lapping machine configuration, in: Solid State Phenomena, 165, Trans Tech Publications Ltd, 2010, pp. 237–243.

[21] M.F. Ismail, K. Yanagi, H. Isobe, Characterization of geometrical properties of electroplated diamond tools and estimation of its grinding performance, Wear 271 (3–4) (2011) 559–564.

[22] H. Li, L. Zou, Z. Li, W. Wang, Y. Huang, Investigation on abrasive wear of electroplated diamond belt in grinding nickel-based superalloys, Int. J. Adv. Des. Manuf. Technol. 121 (7–8) (2022) 4419–4429.

[23] D. Bhaduri, R. Kumar, A.K. Jain, A.K. Chattopadhyay, On tribological behaviour and application of TiN and MoS2-Ti composite coating for enhancing performance of monolayer cBN grinding wheel, Wear 268 (9–10) (2010) 1053–1065.

[24] R.P. Upadhyaya, S. Malkin, Thermal aspects of grinding with electroplated CBN wheels, J. Manuf. Sci. Eng. 126 (1) (2004) 107–114.

[25] Z. Liu, Y. Yang, X. Yang, B. Pan, Influence of zinc sulfate concentration in baths on the structure, morphology and tribocorrosion properties of Fe-Zn alloy coating, Surf. Coating. Technol. 422 (2021), 127561, https://doi.org/10.1016/j.surfcoat.2021.127561.

[26] Z. Shi, S. Malkin, An investigation of grinding with electroplated CBN wheels, CIRP Ann. - Manuf. Technol. 52 (1) (2003) 267–270.

[27] W. Huang, Y. Li, X. Wu, J. Shen, The wear detection of mill-grinding tool based on acoustic emission sensor, Int. J. Adv. Des. Manuf. Technol. (2022) 1–10.

[28] M. Deja, Method of monitoring of the grinding process with lapping kinematics using audible sound analysis, J. Mach. Eng. 22 (2022).

[29] Z. Shi, S. Malkin, Wear of electroplated CBN grinding wheels, J. Manuf. Sci. Eng. 128 (1) (2006) 110–118.

[30] R.P. Upadhyaya, J.H. Fiecoat, Factors affecting grinding performance with electroplated CBN wheels, CIRP Ann.-Manuf. Technol. 56 (1) (2007) 339–342.

[31] M. Deja, Wear of electroplated tools used for flat grinding of ceramics, in: Solid State Phenomena, 199, Trans Tech Publications Ltd, 2013, pp. 633–638.

[32] A. Barylski, M. Deja, Influence of flat lapping kinematics on machinability of ceramics, in: Solid State Phenomena, 199, Trans Tech Publications Ltd, 2013, pp. 615–620.

[33] H. Li, C. Fang, Study on generation of abrasive protrusion height based on projection information–driven intelligent algorithm, Int. J. Adv. Des. Manuf. Technol. 123 (11) (2022) 4309–4320.

[34] M. Deja, D. Zieliński, Wear of electroplated diamond tools in lap-grinding of Al_2O_3 ceramic materials, Wear 460 (2020), 203461.

[35] C.A. Huang, C.H. Shen, P.Y. Li, P.L. Lai, Effect of fabrication parameters on grinding performances of electroplated Ni-B-diamond tools with D150-diamond particles, J. Manuf. Process. 80 (2022) 374–381.

[36] C.A. Huang, C.H. Shen, W.Z. Huang, J.S. Lo, P.L. Lai, Grinding performance of electroplated diamond tools strengthened with Cr-C deposit using D-150 diamond particles, Int. J. Adv. Des. Manuf. Technol. 121 (7–8) (2022) 4549–4558.

[37] H.M. Kim, G.H. Park, Y.G. Seo, D.J. Moon, B.J. Cho, J.G. Park, Comparison between sapphire lapping processes using 2-body and 3-body modes as a function of diamond abrasive size, Wear 332–333 (2015) 794–799.

[38] J. Badger, S. Murphy, G.E. O'Donnell, Big-and-dull or small-and-sharp: a comparison of specific energy, wheel wear, surface-generation mechanisms and surface characteristics when grinding with Al2O3 and CBN to achieve a given surface roughness, J. Mater. Process. Technol. 288 (2021), 116825.

[39] M. Korzyński, „Methodology of the Experiment. Planning, Implementation and Statistical Analysis of the Results of Technological Experiments", Publisher House: Wydawnictwo WNT, Polish, 2013, p. 277, 2018.

[40] L. Guo, R.S. Subramanian, Mechanical removal in CMP of copper using alumina abrasives, J. Electrochem. Soc. 151 (2) (2004) G104–G108.

[41] A. Barylski, N. Piotrowski, Non-conventional approach in single-sided lapping process: kinematic analysis and parameters optimization, Int. J. Adv. Manuf. Technol. 100 (1–4) (2019) 589–598.

[42] J.F.G.D. Oliveira, E.J.D. Silva, C. Guo, F. Hashimoto, Industrial challenges in grinding, CIRP Ann. 58 (2) (2009) 663–680.

11